Journal of Imaging Science and Technology® 67(5): 1–10, 2023.

An Appearance Reproduction Framework for Printed 3D Surfaces

Tanzima Habib, Phil Green, and Peter Nussbaum▲
Department of Computer Science, Norwegian University of Science and Technology (NTNU), Norway
E-mail: syeda.t.habib@ntnu.no

Abstract. *Bidirectional reflection distribution function (BRDF) is used to measure colour with gloss and surface geometry. In this paper, we aim to provide a practical way of reproducing the appearance of a 3D printed surface in 2.5D printing of any slope angle and colour in a colour-managed workflow as a means for softproofing. To account for the change in colour due to a change in surface slope, we developed a BRDF interpolation algorithm that adjusts the colour of the tristimulus values of the flat target to predict the corresponding colour on a surface with a slope. These adjusted colours are then used by the interpolated BRDF workflow to finally predict the colour parameters for each pixel with a particular slope. The effectiveness of this algorithm in reducing colour differences in 2.5D printing has been successfully demonstrated. We then finally show how all the components, slope colour adjustment method, interpolated BRDF parameters algorithm, and BRDF model encoded profiles using iccMAX are connected to make a practical appearance reproduction framework for 2.5D printing.* © *2023 Society for Imaging Science and Technology.*
[DOI: 10.2352/J.ImagingSci.Technol.2023.67.5.050413]

1. INTRODUCTION

Additive manufacturing does not typically have high expectations of colour fidelity. Within the domain of 3D printing, there is a sector which prints low-relief (typically ⇐ 10 mm) samples on a planar base. This is sometimes referred to as "2.5D printing". The users and the technologies in this sector are more akin to graphic technology than additive manufacturing. An example would be a reproduction of a painting, with the relief's ability to reproduce the spatial characteristics of the artist's brushwork. Relief prints could possibly be colour characterised by the same methods as in 2D printing. However, as the angle to the planar surface normal changes, the colour can undergo a change due to the voxel structure and in particular, the dot placement. Page et al. discussed how the height printed is affected by different printing parameters such as ink colour, ink droplet size, UV curing time, printing direction etc. Since printing parameters affect height generation and surface roughness naturally this in turn impacts the surface colour [1]. Song et al. showed how four-flux transfer model can be used to predict colour of inks printed with different thicknesses [2]. Such characterization methods in the case of complete planar colour reproduction involve the measurement of a large sample of colorant combinations and with different printed heights or slopes, this requirement of sample measurement increases. However, it is impractical to measure and characterise colour for every changing slope, therefore a smart way of predicting colour for changing slope with minimal colour measurements is required.

In addition, in a reproduction workflow, the user may prefer to preview the final reproduction at different illumination and viewing angles. The appearance of a 3D object can be predicted by a bidirectional reflectance distribution function (BRDF) model. BRDF defines how light is reflected off the surface in different directions according to the angle of incidence and the angle of reflection [3]. In computer graphics, the 3D rendering on a display is the final output and as there is no reference, a reasonable degree of visual realism is usually acceptable. In relief (2.5D) printing, it is important that the final output matches the preview seen on a display, and this also requires integration into a colour-managed workflow with accurate display calibration and the ability to exchange appearance data through the workflow. Therefore, softproofing is an important tool for controlling print properties such as colour, glossiness, and texture with high accuracy. It allows users to accurately represent the desired appearance attributes of the object and to make adjustments as needed before printing, ensuring that the final product meets their specifications. This process is already a widely used standard practice in commercial and industrial 2D digital printing, where accurate print preview is critical, as it helps designers and product owners visualise the end product and make adjustments as needed before printing, ensuring that the final product meets their specifications. However, such softproofing through colour management for relief surfaces is challenging and has not been utilised in a 2.5D printing pipeline. Softproofing in 3D printing involves generating a visual preview of the appearance of a 3D printed object using CAD software tools to assess and modify attributes such as colour, surface texture, and translucency. HP developed a 3D printing softproofing system that has an Appearance Reference Object (ARO) integrated. An ARO demonstrates the printing system's colour capabilities using 3D sub-objects. It has flat and curved surfaces that showcase the effects of colour orientation. The softproofing system allows designers to view and modify the simulated ARO [4]. In the case of 2.5D printing, an attempt towards 2.5D softproofing is achieved

▲ IS&T Member.

Received June 5, 2023; accepted for publication Aug. 29, 2023; published online Oct. 19, 2023. Associate Editor: Kye Si Kwon.

1062-3701/2023/67(5)/050413/10/$25.00

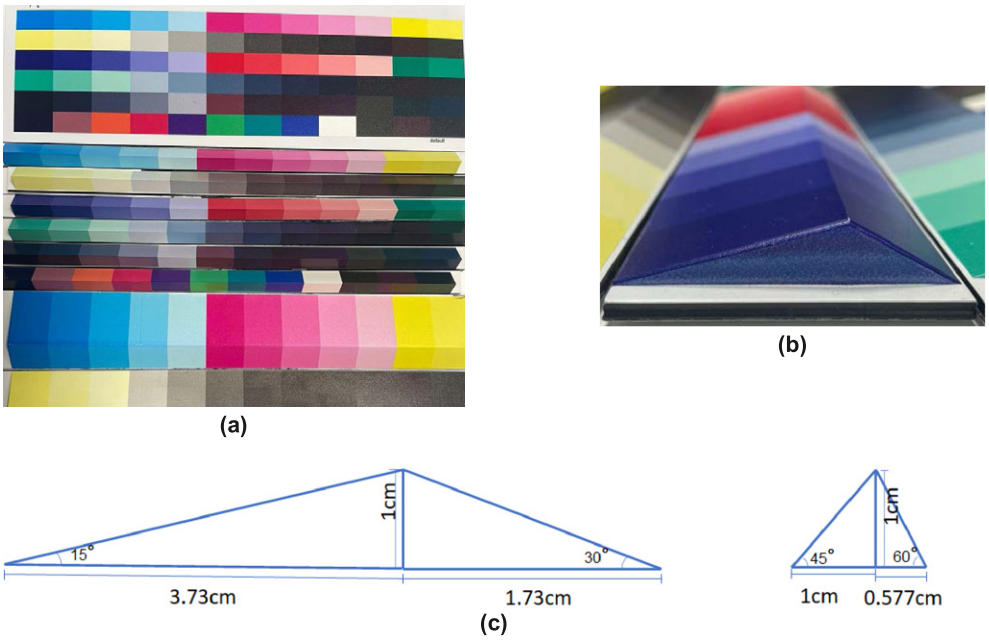

Figure 1. Printed 2.5D target samples.

through the use of a colour prediction model based on the four-flux theory mentioned earlier, which accurately predicts the reflectance and transmittance of ink slabs of different thicknesses for the primary colourants of the printer [2]. Moreover, Piovarci et al. showed that by controlling the halftoning algorithm of varnish the gloss reproduction can be handled which is a challenging task in current printing systems [5]. Therefore, in softproofing of 2.5D printed surface, it is important to capture inaccuracies of a particular system which affects the final appearance along the surface created with variable height. Hence the goals of this work are: (a) a BRDF model that works with minimal data and (b) implementation in an open colour management framework, for a 2.5D printed surface of any colour and slope angle. This should enable the prediction of colorant amounts to reproduce a given appearance and an accurate real-time preview that can be updated dynamically as the viewing configuration changes.

2. METHODS

In this section, we first describe the development of an efficient method of implementing a BRDF model. This extends our previous work on interpolating BRDF parameters from a minimal number of measurements, which we fit to a suitable BRDF model. Second, we describe the implementation of the model in a reproduction framework using the ICC.2 colour management architecture. Section 2.3 Appearance Reproduction Framework describes the steps involved to achieve these aims.

2.1 *2.5D Printed Target Samples*

Colour patches were printed on a substrate using a 2.5D inkjet printer. The patches were printed flat on the substrate and on four different slopes with angles of 15°, 30°, 45°, and 60°, as illustrated in Figure 1(c). For each slope, a total of 72 colour patches of the FOGRA Media Wedge CMYK V3.0 were printed, including a flat print, which is shown in Fig. 1(a). Fig. 1(b) displays the side view of the colour patches printed on slopes of 15° and 30°, respectively. In total, 360 colour patches were printed.

2.2 *Measurements*

For each type of surface, i.e., flat, 15°, 30°, 45°, and 60° slopes, 23 colour samples were selected from the 72 colour patches. The BRDF of the eight primary and secondary samples, as well as the nine test samples, was measured using a GON 360 goniometer equipped with a CAS 140CT array spectrophotometer. Measurements were carried out at incidence angles (θ_i) of 0°, 15°, 30°, 45°, and 60°, and viewing angles (θ_r) ranging from 30° to −65° in 5° intervals with respect to the incidence angle space. In total, 65 reflectance measurements for each colour patch were carried out.

2.3 *Appearance Reproduction Framework*

In this section, we discuss the aim to develop a step-wise appearance reproduction framework for 2.5D printing. Our goal is to create a workflow that can produce BRDF parameters for an image with *XYZ* values measured at 0°:45° geometry, which is an image containing the in-gamut *XYZ* values produced by applying a printer profile. This printer profile is created using a flat printed target, traditionally measured and modelled in printer colour management.

In a previous work [6], we developed a similar workflow to predict BRDF parameters from *XYZ* values for 2D printing. This method uses an interpolation algorithm that uses *XYZ* values and optimised BRDF parameters of the

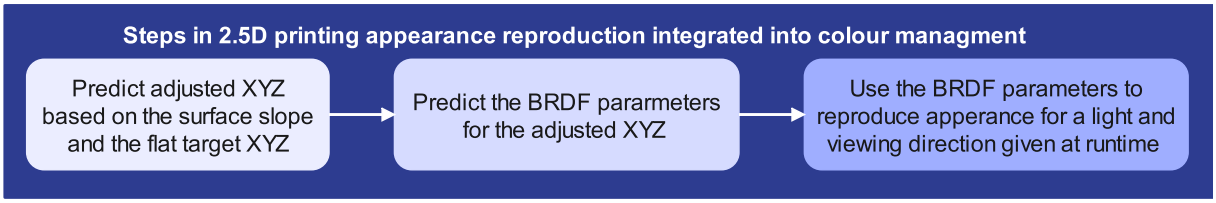

Figure 2. Steps in appearance reproduction integrated into colour management for 2.5D printing.

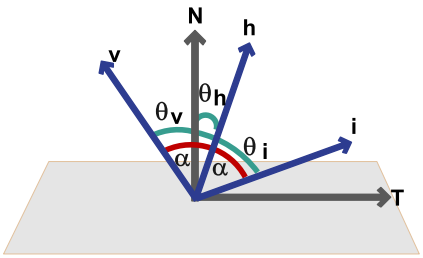

Figure 3. Diagram of half-angle vector, incidence direction, viewing direction and normal.

primary and secondary printed colours of a specific printer and substrate to predict the BRDF parameters given an *XYZ* value. This algorithm is discussed in Section 2.5.

In the context of 2.5D printing, which involves printing on surfaces with spatially variable heights, it is important to note that the colorimetry of device colours may differ when printed on surfaces with different slopes compared to a flat surface. This discrepancy arises due to the subtle differences in the structure deposition and layering of coloured inks on surfaces with varying height, resulting in distinct surface structures that affect colour appearance. As a result, when performing softproofing, which aims to simulate the appearance of printed colours on a display, it is crucial to account for the colour changes associated with changes in surface slope. Thus, when softproofing, it becomes important to consider the impact of changes in surface slope on colour changes. Nonetheless, the task of modelling the BRDF of every surface with a distinct slope and colour would be impractical. Therefore, alternative methods need to be developed to account for these effects in the appearance reproduction of 2.5D printed surfaces.

We propose using BRDF of the primary and secondary colours of the 2.5D printed flat target and interpolating them to predict the BRDF parameters of surfaces with slopes greater than 0°. We will adjust for the diffuse colour change between the flat target and the sloped surface. For softproofing, slope information can be retrieved from a normal map. Therefore, we have developed a colour adjustment algorithm that adjusts the colour of the tristimulus values of the flat target to predict the corresponding tristimulus value on a surface with some slope. These adjusted colours are then used by the interpolated BRDF parameters algorithm to finally predict the BRDF parameters for each pixel with a particular slope. The output will be an image with channels that have the BRDF parameters and the surface normals from the normal map. This output can be used by modifying the integrated BRDF colour management rendering workflow developed in a previous work [7] discussed in Section 2.3.

The new modified workflow uses multiplex connection space ICC profiles with an encoded BRDF model that can be applied to BRDF parameters and surface normals file to get the tristimulus values at a given light and viewing direction. The global light and viewing direction are passed at run-time in this workflow. Furthermore, a display profile can be applied to the *XYZ* output for visualisation.

Therefore, to summarise, the appearance reproduction framework will have the following steps for a given in-gamut *XYZ* values and its surface normals: (1) adjust the *XYZ* value of the flat target based on the slope of the surface extracted from the surface normals, (2) predict BRDF parameters of these adjusted colours using the interpolated BRDF parameter algorithm, and (3) apply a BRDF rendering workflow using iccMAX to generate *XYZ* values from the BRDF parameters at a given light and viewing direction. The steps in the proposed appearance reproduction framework for 2.5D printing softproofing are shown in Figure 2.

2.4 *BRDF Optimisation*

In BRDF optimisation, the Cook-Torrance model is employed. This BRDF model is based on the microfacet theory and is grounded on physically-based assumptions. The model postulates that the microfacets oriented towards the half-angle vector contribute to the final reflection. To generate the specular term, the model uses three critical concepts: a distribution term D, which characterises the distribution of microfacets; a Fresnel term F, which determines the reflection behaviour of each microfacet; and a geometric attenuation factor G, which accounts for the shadowing and masking of one microfacet by another [8].

The Fresnel term is determined using Schlick's approximation [9], which is shown in Eq. (1). Here, n represents the refractive index of the material. D and G terms are shown in Eq. (2). θ_i, θ_v and θ_h are the angles between incidence direction vector **i**, viewing direction vector **v** and the half vector **h** with the normal N respectively as shown in Figure 3. To describe D, a Gaussian distribution is utilised, which incorporates the parameter m. In G, angle α refers to the angle between the viewing direction vector **v** and the half-angle vector **h** as shown in Fig. 3.

The first version of the Cook-Torrance model is shown in Eq. (3). This model optimises the diffuse component

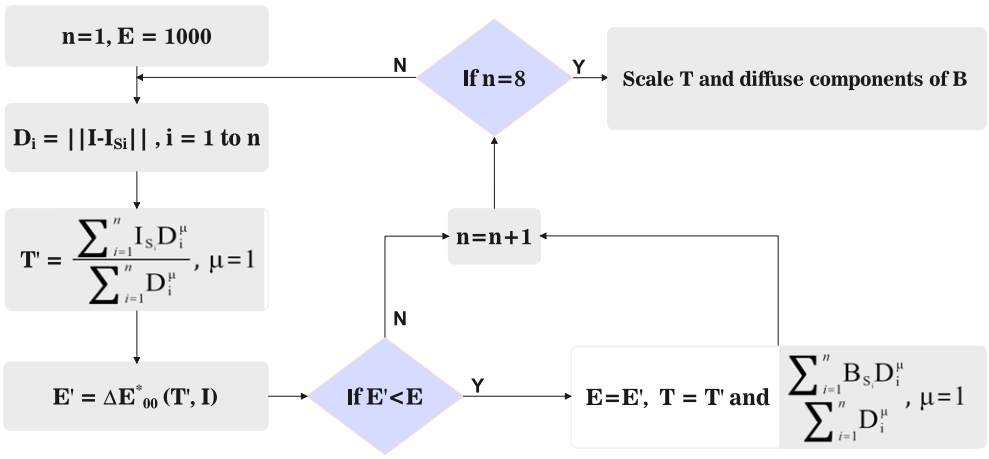

Figure 4. Flowchart of steps 1 to 6 of interpolated BRDF parameters algorithm.

kd_x, kd_y, kd_z and specular component k_{sj}, where $j = 1 \ldots 3$, for each colour channel X, Y, and Z and R_s is given in Eq. (4). The second version of the model, as shown in Eq. (5), optimises m_j, where $j = 1 \ldots 3$, the parameter that describes the specular lobe, for each channel. Consequently, we obtain R_{s1}, R_{s2}, and R_{s3} for each channel, as shown in Eq. (6) by using Eq. (7). kd_x, kd_y, and kd_z are the diffuse components, and m is the parameter that controls the specular lobe. Therefore, the first version of the Cook-Torrance model has seven parameters, which we call BRDF1, while the second version has nine parameters, which we call BRDF2. For the optimisation of BRDF, we chose two different cost functions, RMSE which is one of the commonly used metrics to optimise BRDF [10] and ΔE^*_{00} which is a perceptual metric. We optimise BRDF1 with rmse and call it BRDF1 RMSE and both BRDF1 and BRDF2 are optimised with ΔE^*_{00} and call them BRDF1 CD and BRDF2 CD respectively.

$$R_o = \left(\frac{1-n}{1+n}\right)^2, \quad F = R_o + (1-R_o)(1-\cos\theta_i)^5 \tag{1}$$

$$D = \frac{\exp^{-\left[\frac{\tan\theta_h}{m}\right]^2}}{m^2\cos^4\theta_h}, \qquad G = \min\left\{1, \frac{2\cos\theta_h\,\cos\theta_i}{\cos\alpha}, \frac{2\cos\theta_h\,\cos\theta_v}{\cos\alpha}\right\} \tag{2}$$

$$\begin{bmatrix} I_x \\ I_y \\ I_z \end{bmatrix} = I_i \cos\theta_i \left(\frac{1}{\pi}\begin{pmatrix} kd_x \\ kd_y \\ kd_z \end{pmatrix} + \begin{pmatrix} ks_1 \\ ks_2 \\ ks_3 \end{pmatrix} R_s\right) \tag{3}$$

$$R_s = \frac{FDG}{\pi\cos\theta_i\,\cos\theta_v} \tag{4}$$

$$D_1 = \frac{\exp^{-\left[\frac{\tan\theta_h}{m_1}\right]^2}}{m_1^2\cos^4\theta_h}, \quad D_2 = \frac{\exp^{-\left[\frac{\tan\theta_h}{m_2}\right]^2}}{m_2^2\cos^4\theta_h} \quad \text{and} \quad D_3 = \frac{\exp^{-\left[\frac{\tan\theta_h}{m_3}\right]^2}}{m_3^2\cos^4\theta_h} \tag{5}$$

$$\begin{bmatrix} I_x \\ I_y \\ I_z \end{bmatrix} = I_i \cos\theta_i \left(\frac{1}{\pi}\begin{pmatrix} kd_x \\ kd_y \\ kd_z \end{pmatrix} + \begin{pmatrix} ks_1 R_{s1} \\ ks_2 R_{s2} \\ ks_3 R_{s3} \end{pmatrix}\right) \tag{6}$$

$$R_{st} = \frac{FD_t G}{\pi\cos\theta_i\,\cos\theta_v}, \quad t = 1 \cdots 3 \tag{7}$$

2.5 *Interpolated BRDF*

In this section, we describe the interpolated BRDF parameters algorithm [6], flowchart of steps 1 to 6 of this algorithm is shown in Figure 4.

Let the input tristimulus value be the vector **I**, and the tristimulus values of the eight primary and secondary colours be the vectors $\mathbf{I}_i$ and their corresponding BRDF parameters be the vectors $\mathbf{B}_i$ where $i \in 1, 2, 3, \ldots, 8$ and $\mathbf{B}_i \in R^q$ where q is the number of BRDF parameters in the chosen BRDF model.

Calculate the chromaticity coordinate vector **C** of **I** and the chromaticity coordinate vectors $\mathbf{C}_i$ of $\mathbf{I}_i$, respectively, where $i \in 1, 2, 3, \ldots, 8$. For a given tristimulus value, the chromaticity coordinates x, y, z are given by:

$$x = \frac{X}{X+Y+Z}, \quad y = \frac{Y}{X+Y+Z}, \quad z = \frac{Z}{X+Y+Z}. \tag{8}$$

Then, we find the distance between the vectors **C** and $\mathbf{C}_i$ based on the L_p norm as follows: $\mathbf{D}_i = ||\mathbf{I} - \mathbf{I}_{S_i}||_p$, where p can be chosen accordingly, and in this case we choose $p = 2$ which reduces it to the Euclidean distance.

We create vectors $\mathbf{S}_i$ that store the index i of $\mathbf{d}_i$ in ascending order of distance values in the vector $\mathbf{d}_i$, where i changes from 1 to 8.

Next, we set $n = 1$ and perform the following steps:

1. Set the variable of the colour difference $\boldsymbol{E} = 1000$.
2. Calculate the distance $\boldsymbol{D_i} = \left|\left|\boldsymbol{I} - \boldsymbol{I}_{S_i}\right|\right|$, where i changes from 1 to n.
3. Calculate the tristimulus value $\boldsymbol{T}$ as: $\boldsymbol{T} = \frac{\sum_{i=1}^{n} \boldsymbol{I}_{S_i} \boldsymbol{D}_i^{\mu}}{\sum_{i=1}^{n} \boldsymbol{D}_i^{\mu}}$, where μ can be chosen accordingly, and in this case we choose $\mu = 1$.

4. Calculate the colour difference $\boldsymbol{E}'$ using ΔE^*_{00} between $\boldsymbol{T}'$ and $\boldsymbol{I}$.
5. If $\boldsymbol{E}' < \boldsymbol{E}$, then set $\boldsymbol{E} = \boldsymbol{E}'$, interpolated tristimulus vector $\boldsymbol{T} = \boldsymbol{T}'$, and calculate interpolated BRDF parameters vector $\mathbf{B}$ as: $\mathbf{B} = \frac{\sum_{i=1}^{n} \boldsymbol{B}_{S_i} \boldsymbol{D}_i^{\mu}}{\sum_{i=1}^{n} \boldsymbol{D}_i^{\mu}}$.
6. Increment n and repeat steps 2 to 5 until $n = 8$.

Once we find the closest tristimulus value $\boldsymbol{T}$ and the corresponding BRDF parameters $\mathbf{B}$, we then need to scale each tristimulus coordinate $(\boldsymbol{T}_x, \boldsymbol{T}_y, \boldsymbol{T}_z)$ of $\boldsymbol{T}$ to match the tristimulus coordinates $(\boldsymbol{I}_x, \boldsymbol{I}_y, \boldsymbol{I}_z)$ of $\boldsymbol{I}$, and we apply the same scaling to the diffuse components $(\boldsymbol{kd}_x, \boldsymbol{kd}_y, \boldsymbol{kd}_z)$ of $\mathbf{B}$.

To achieve this, we calculate the scaling factors for each coordinate, denoted as a, b, and c, respectively:

$$a = \frac{\boldsymbol{I}_x}{\boldsymbol{T}_x},\ b = \frac{\boldsymbol{I}_y}{\boldsymbol{T}_y} \text{ and } c = \frac{\boldsymbol{I}_z}{\boldsymbol{T}_z}$$

Finally, we apply the scaling factors $\boldsymbol{a}$, $\boldsymbol{b}$, and $\boldsymbol{c}$ to get $\boldsymbol{T} = (\boldsymbol{I}_x, \boldsymbol{I}_y, \boldsymbol{I}_z)$ and the diffuse component of the BRDF is $\boldsymbol{B} = (a\boldsymbol{kd}_x, b\boldsymbol{kd}_y, c\boldsymbol{kd}_z)$.

2.6 *2.5D Slopewise Colour Adjustment*

To adjust the tristimulus value of a flat target colour patch to obtain the corresponding colour on a sloped surface, a colour adjustment algorithm has been developed that uses the tristimulus values of the white and black primary colour patches printed on the sloped surfaces. The algorithm is given below where W_f and B_f are the tristimulus values of the white and black colour patches of the flat target measured with 0°:45° geometry, W_s and B_s are the tristimulus values of the white and black colour patches of the sloped surface measured with 0°:45° geometry to their surface normal, given any tristimulus value T_f of the flat target, the tristimulus value of the sloped surface T'_s in the same geometry can be predicted as given in Eqs. (9)–(12). L_{T_f}, L_{W_f} and L_{B_f} are the lightness values of T_f, W_f and B_f, respectively. Therefore, this method requires printing and measuring white and black colour patches for a number of sloped surfaces whose values can be used to find values of intermediate slopes using interpolation.

$$C = \frac{W_s - B_s}{W_f - B_f} \tag{9}$$

$$T'_s = (T_f - CB_f)\frac{W_s}{W_f} + CB_s \quad \text{for} \quad L_{T_f} < L_{W_f} \quad \text{and} \quad L_{T_f} > L_{B_f} \tag{10}$$

$$T'_s = T_f \frac{W_s}{W_f} \quad \text{for} \quad L_{T_f} \geq L_{W_f} \tag{11}$$

$$T'_s = (T_f - CB_f) + CB_s \quad \text{for} \quad L_{T_f} \leq L_{B_f}. \tag{12}$$

2.7 *Colour Management Integrated BRDF Rendering*

In this section, we describe an iccMAX colour management framework to transform input *XYZ* data to a simulation of the directional appearance on a display, which is useful for softproofing. This workflow is a modification to handle BRDF parameters along with a normal map, compared to a previous workflow developed in Ref. [7]. The core task is to transform from an *XYZ* space representing diffuse reflectance (0°:45° geometry) to an adjusted *XYZ* representing the appearance of the material once the angles of light and viewing directions are given. However, the ICC.1 colour management architecture has its limitations in handling such transformations, as it specifies a point-wise transform with a restricted set of transform elements. Moreover, PCS (profile connection space) represents a matte, diffusely reflecting planar surface that is measured using a 0°:45° geometry and under D50 illuminant colorimetry [11].

To tackle this limitation, the ICC.2 architecture, i.e. iccMAX, is employed. It extends the ICC.1 architecture and provides much more comprehensive support for the colour management of various types of materials and geometries of measurement. The iccMAX framework supports a broader range of transform elements, as well as fully directional illumination, measurement, and viewing geometries [12]. Furthermore, it incorporates an option to utilise Calculator Element Programming, a scripting language that enables fully programmable transforms [13].

In this colour management workflow, the BRDF model is encoded in a Calculator Elements tag within the main function, using a framework called multiplex connection space (MCS). The MCS framework consists of two profiles: Multiplex Identification (MID) and Multiplex Visualisation (MVIS) profiles. The parameters optimised for the BRDF model and the surface normals for each pixel are transmitted through the input channels to the MID profile and then used by the BRDF model encoded in the MVIS profile. The light and viewing directions are sent as run-time variables to the MVIS profile. The MVIS profile processes the input and employs the encoded BRDF model to produce the *XYZ* values in the appropriate light and viewing geometry. The output channels containing the rendered *XYZ* values are then passed through the MVIS profile, which connects them to the colorimetric PCS, carrying out any processing required to convert them to this PCS. Multiplex Type Array Tags are established to assign channel names and are employed to match channels in and out of the MCS, and to verify channel compliance with any subset requirements between profiles. The optional Multiplex Default Values Tag defines the default values for channels. The MID profile uses an AToM0 tag to provide the transformation from device channel data to MCS channel data, while the MVIS class profile employs MToB0 (colorimetric) tags to provide the transformation from MCS channel data to PCS channel data. Finally, a display profile can be applied for visualisation on a screen.

2.8 *Tests*

For the purpose of testing, 15 out 23 colour patches were used whose BRDF parameters were obtained by fitting a BRDF model to their BRDF measurements. The BRDF parameters obtained as such form the reference values for the predicted BRDF parameters using our slope-colour adjusted

Table I. Colour difference between the 23 colour patches printed on the flat substrate and the colour patches printed on a sloped surface of 15°, 30°, 45° and 60° angles, (a) each measured at 0°:45° geometry, (b) each slope colours obtained from adjusting the flat colours.

	Flat versus Slope 15°	Flat versus Slope 30°	Flat versus Slope 45°	Flat versus Slope 60°
Mean ΔE^*_{00} (a)	1.14	2.35	6.45	4.86
Mean ΔE^*_{00} (b)	0.95	1.50	3.66	3.15
Max ΔE^*_{00} (a)	3.28	3.80	8.92	9.56
Max ΔE^*_{00} (b)	2.87	4.03	6.18	6.99

and interpolated BRDF parameter workflow tailored for 2.5D printing, which we call the adjusted interpolated BRDF (AIB). We also predict the BRDF parameters using the interpolated BRDF parameters workflow without any colour adjustment for the surfaces with varying slopes; we call it interpolated BRDF (IB). We compare the colour difference between the tristimulus values obtained using the optimised BRDF (BRDF1 CD) and the corresponding tristimulus values from methods IB and AIB respectively. And then show how all the component workflows and algorithms discussed make a practical appearance reproduction framework for 2.5D printing.

3. RESULTS AND DISCUSSION

Table I(a) shows the mean and maximum ΔE^*_{00} obtained between the 23 colour patches printed on the flat substrate and the colour patches printed on a sloped surface of 15°, 30°, 45° and 60°, respectively, each measured at 0°:45° geometry. It can be seen that the mean and max ΔE^*_{00} increase as the slope increases. Slope 45° has the most colour inconsistency with respect to the flat target. In an ideal case, the colours on the sloped surfaces should have matched the colours on the flat target. Therefore, this establishes the need for a colour adjustment algorithm to predict the colours of the sloped surfaces from the colours of the flat target. Table I(b) shows the mean and max ΔE^*_{00} obtained for the 23 colour patches after the colour adjustment. It can be seen that both mean and maximum ΔE^*_{00} are lower for the adjusted colours except for the maximum value of flat vs. slope 30°. 15° and 30° slopes have maximum colour difference with the flat target less than $5\Delta E^*_{00}$, also the improvements, in this case, are negligible, less than $1\Delta E^*_{00}$. While in the case of 45° and 60° slopes have significantly higher colour differences and the improvement achieved by adjusting colour is also significant, around $3\Delta E^*_{00}$ and $1.5\Delta E^*_{00}$ improvement for the mean respectively. For colour difference of less than $5\Delta E^*_{00}$, we consider $1\Delta E^*_{00}$ improvement significant, for colour difference between $5\Delta E^*_{00}$ and $10\Delta E^*_{00}$ and we consider $2\Delta E^*_{00}$ improvement significant, for higher colour differences.

Table II shows the colour difference between the measured BRDF and the optimised BRDF (BRF1 CD) results obtained for the primary and secondary colours of the flat target. The mean ΔE^*_{00} is obtained between the measured tristimulus values of the flat target and its optimised BRDF tristimulus values for different combinations of angle of incidence and reflection for each primary and secondary colour. For BRDF modelling, two versions of the Cook-Torrance BRDF model were used - one with seven parameters (BRDF1) and another with nine parameters (BRDF2). Further, for optimisation, two metrics were used for BRDF1 rmse and ΔE^*_{00} and for BRDF2 only ΔE^*_{00} was used and they are called BRDF1 RMSE, BRDF1 CD and BRDF2 CD, respectively. Table II shows that BRDF1 RMSE has inconsistent high colour differences for diffuse and near-specular colours. Also, BRFD1 RMSE performs the worst among the three BRDF versions in predicting diffuse and near-specular colours. It has been found that BRDF1 RMSE can lead to high hue shifts while BRDF1 CD and BRDF2 CD tend to preserve hue at the cost of chroma and lightness, although BRDF1 RMSE predicts the specular peaks better than BRDF1 CD. Figure 5 is a visual representation of BRDF1 RMSE (top), measured BRDF (middle) and BRDF1 CD (bottom) for different angles of incidence and viewing of two colours showing the visible hue shifts in the case of BRDF1 RMSE. Such hue shifts are not desired in softproofing of a material. From the table, it can also be seen that there is no significant difference in using the BRDF2 CD model with nine parameters. BRDF parameters will be used as channel values for images in an appearance reproduction framework. Therefore, to limit the number of BRDF parameters, we carry forward our framework with the BRDF1 CD model with seven parameters.

Table III shows the colour difference between the tristimulus values of the optimised BRDF (BRDF1 CD) of the colours on each slope and the interpolated BRDF (IB) of the flat target; the colour difference between the tristimulus values of optimised BRDF (BRDF1 CD) of the colours on each slope and its corresponding slope colour adjusted interpolated BRDF (AIB) of the flat target. Optimised BRDF (BRDF1 CD) of the sloped surface colours is the reference in this case and we compare the performance of the IB and AIB methods using the optimised BRDF of the primary and secondary colour of the flat target in predicting the slope BRDF. These colour differences are quantified on the basis of three regions, namely diffuse reflection, specular reflection and near-to-specular reflection. Specular reflection is the case when the angle of reflection is a perfect mirror angle of the angle of incidence. We defined near-to-specular reflection in this case, as the region 15°

Table II. Colour difference between the reference and optimised BRDF (BRDF1 CD) results of the primaries and secondaries of the flat target at different incidence and reflection angles.

		C100	M100	Y100	B100	G100	R100	K100	White	Average
Diffuse	Mean ΔE^*_{00} BRDF1 CD	6.09	5.10	5.94	4.90	5.29	6.02	6.20	5.84	5.67
	Mean ΔE^*_{00} BRDF1 RMSE	7.48	7.50	6.94	7.19	9.10	7.45	*16.04*	**6.50**	**8.52**
	Mean ΔE^*_{00} BRDF2 CD	5.86	4.89	5.89	4.56	5.14	5.15	3.82	5.84	5.14
	Max ΔE^*_{00} BRDF1 CD	16.59	13.28	15.40	15.39	13.19	14.82	*22.57*	13.10	15.54
	Max ΔE^*_{00} BRDF1 RMSE	16.21	15.64	14.31	*21.72*	16.47	16.14	*21.70*	14.18	**17.05**
	Max ΔE^*_{00} BRDF2 CD	14.67	13.03	15.29	12.91	14.43	10.52	14.47	13.00	13.54
Specular	Mean ΔE^*_{00} BRDF1 CD	2.95	3.79	2.00	8.58	4.01	4.74	3.94	0.37	**3.80**
	Mean ΔE^*_{00} BRDF1 RMSE	2.16	2.92	1.66	3.56	2.33	1.97	3.38	0.94	2.37
	Mean ΔE^*_{00} BRDF2 CD	2.20	2.46	1.72	5.31	2.32	1.94	2.58	0.38	2.36
	Max ΔE^*_{00} BRDF1 CD	5.38	5.79	3.82	12.97	6.05	7.73	6.12	0.95	**6.10**
	Max ΔE^*_{00} BRDF1 RMSE	2.81	3.66	1.91	5.81	3.13	2.71	4.55	1.61	3.27
	Max ΔE^*_{00} BRDF2 CD	4.50	4.31	2.77	9.88	4.64	3.41	4.42	0.97	4.36
N-Specular	Mean ΔE^*_{00} BRDF1 CD	2.48	2.48	1.97	3.96	3.35	3.32	2.98	1.73	2.78
	Mean ΔE^*_{00} BRDF1 RMSE	3.30	4.20	2.35	9.94	6.07	4.87	3.71	2.04	**4.56**
	Mean ΔE^*_{00} BRDF2 CD	2.51	2.05	2.13	3.75	2.94	2.91	2.72	2.08	2.64
	Max ΔE^*_{00} BRDF1 CD	5.14	4.97	4.67	8.90	6.17	6.83	9.50	5.48	6.46
	Max ΔE^*_{00} BRDF1 RMSE	11.49	12.73	6.87	*38.38*	*22.01*	*19.59*	6.19	5.52	**15.35**
	Max ΔE^*_{00} BRDF2 CD	5.38	4.99	7.24	8.82	6.44	6.65	11.10	9.35	7.49

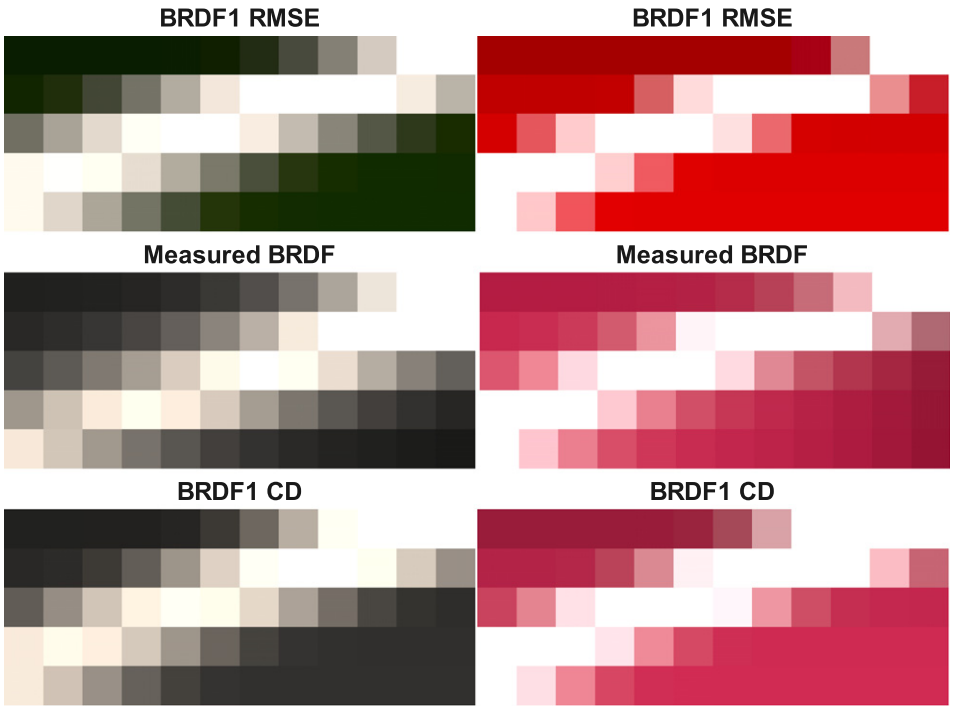

Figure 5. Visual representation of BRDF1 RMSE, Measured RMSE and BRDF1 CD for different angles of incidence and viewing for two printed colours.

around the specular reflection where both material colour and the illuminant colour mix. The specular lobe observed in this case is broader than the specular lobe obtained previously for glossy 2D printed samples [6]. Therefore, we had to choose a broader near-to-specular region. The rest of the regions fall under diffuse reflection where the material colour is dominant. It can be seen that for all cases except for specular reflections, the AIB method minimises the mean ΔE^*_{00}, although this improvement for mean values is not significant. For each colour patch, there are 68 different

Table III. Colour difference between optimised BRDF (BRDF1 CD) results and the interpolated BRDF parameters algorithm (IB) and adjusted interpolated BRDF parameters algorithm (AIB) for 15 test colour patches at different incidence and reflection angles for each slope.

BRDF1	Diffuse		Specular		Near-to-Specular	
2–5 Slope 15°	IB	AIB	IB	AIB	IB	AIB
Optimised BRDF1 (BRDF1 CD)	2.99	2.33	5.97	5.60	4.87	3.99
Slope 30°	IB	AIB	IB	AIB	IB	AIB
Optimised BRDF1 (BRDF1 CD)	3.54	3.25	3.38	3.80	3.27	3.78
Slope 45°	IB	AIB	IB	AIB	IB	AIB
Optimised BRDF1 (BRDF1 CD)	5.40	5.27	3.63	4.63	4.31	3.76
Slope 60°	IB	AIB	IB	AIB	IB	AIB
Optimised BRDF1 (BRDF1 CD)	4.37	3.93	4.40	4.94	4.43	3.83

Table IV. Colour difference between optimised BRDF (BRDF1 CD) results and interpolated BRDF parameters algorithm (IB) and adjusted interpolated BRDF parameters algorithm (AIB), respectively, for 15 test colour patches at different incidence and reflection angles for all slopes toegther.

	Mean ΔE^*_{00}		Median ΔE^*_{00}		Max ΔE^*_{00}	
	IB	AIB	IB	AIB	IB	AIB
Optimised BRDF1 (BRDF1 CD)	4.39	3.95	4.46	3.84	18.97	14.23

combinations of angle of incidence and reflection out of which only 4 of them are specular reflections, while 16 of them are near-specular-reflections. The colour difference value for high reflectance values at specular angles may not necessarily correspond to the perceived colour difference in the same way it corresponds to the perceived colour difference of diffuse reflections, although it does provide a means of quantification. Table IV shows the grand mean, median, and maximum ΔE^*_{00} considering all the test colour patches of all slopes together. It is observed that the lowest ΔE^*_{00} values are obtained for AIB method. Mean and median colour difference improvements are not significant but the maximum value is minimised by approximately $4.5\Delta E^*_{00}$.

Similarly, from the interpretation of the histograms of these two groups of ΔE^*_{00} values of all the colours of all the slopes for the two methods IB and AIB, it can be established that the frequency distribution of AIB shown in Figure 6(b) has moved towards the lower ΔE^*_{00}, especially the number of samples lower than ΔE^*_{00} of 6 increases significantly compared to the frequency distribution of IB shown in Fig. 6(b). Also, the maximum ΔE^*_{00} has been reduced to 14.23. The Wilcoxon signed rank test was performed on these two groups of ΔE^*_{00} values, which showed that there is a significant difference between the median values of these two methods. Therefore, it can be said that the AIB workflow improves the prediction of BRDF of surfaces with different slopes using the BRDF of the flat target and especially reduces the higher colour differences.

It is important to note that the dataset used was printed in one direction. As the printing method changes, for example, the direction of printing in the xy-plane will affect the quality of the printed surface. Page et al. found that printing in y direction increased printing by 20μ than compared to x-direction [1]. This surface deterioration will in turn impact the slope colours. Therefore, based on the direction of printing, colour correction might be needed. Testing will be required to establish the significance of colour differences due to the change in direction for different slopes, limitations in printing them, and the requirement of adjusting colours further for appearance reproduction.

Based on the results obtained, either IB or AIB method can be used to predict the BRDF parameters for a TIFF file containing *XYZ* values and surface normals from a normal map to retrieve the slope information for each pixel and apply the adjusted colour algorithm accordingly. The output will be a TIFF file containing the BRDF parameters along with the surface normals. Then the MCS profiles encoded with the BRDF model using iccMAX can be used to perform BRDF rendering to the TIFF file that holds the pixel-wise BRDF parameters. Using these profiles, the material appearance can be reproduced for any global light and viewing direction passed at run-time to this colour management pipeline. The output at the end of this pipeline will be a TIFF file containing *XYZ* values at a given light and viewing direction w.r.t. the spatially varying height of the surface translated by the surface normals. For visualisation, a display profile can be applied. This appearance reproduction framework is shown in Figure 7.

4. CONCLUSION

We presented a framework for appearance reproduction in 2.5D printing. The framework uses an interpolation method to predict BRDF parameters for an image with *XYZ* values measured at 0°:45° geometry. To account for the change in colour due to the change in surface slope, we developed a colour adjustment algorithm that adjusts the colour of the tristimulus values of the flat target to predict the corresponding tristimulus value on a surface with some slope.

The comparison of the colour difference between the tristimulus values obtained using the optimised BRDF (BRDF1 CD) and corresponding tristimulus values from methods IB and AIB respectively indicate that the AIB method reduces the mean ΔE^*_{00} for all cases except for specular reflections which are only a handful, although the mean improvement is not significant. However, it reduces colour differences greater than 6 ΔE^*_{00} significantly. Therefore, the effectiveness of this adjusted interpolated BRDF (AIB) workflow in minimising higher colour differences can be useful in 2.5D printing, but if the mean colour difference is of only concern then using IB method is enough.

Moreover, a colour difference metric that is optimised to predict 3D surface colour should be considered for the evaluation of printed slopes since the perception of a 3D surface is affected by the shape, gloss, roughness etc. All

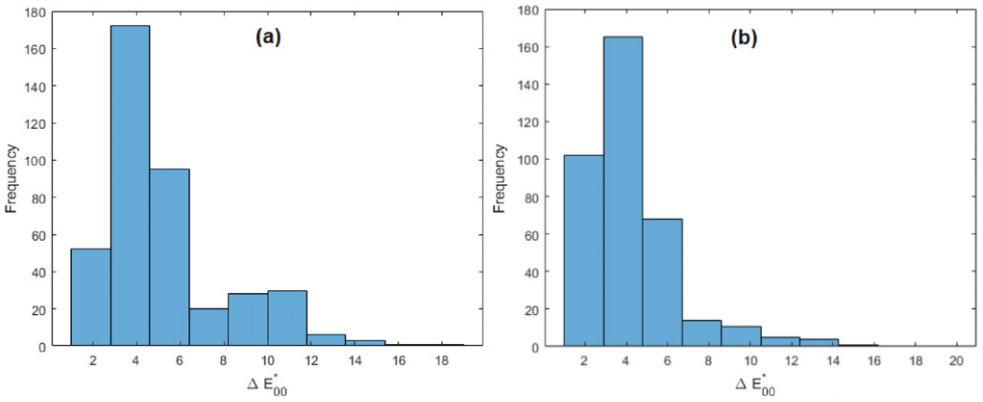

Figure 6. Histogram of colour difference between reflectances obtained for different angles of incidence and reflection of colour samples for all the slopes together (a) ΔE^*_{00} of Optimised BRDF (BRDF1 CD) versus IB results and (B) ΔE^*_{00} of Optimised BRDF (BRDF1 CD) versus AIB results.

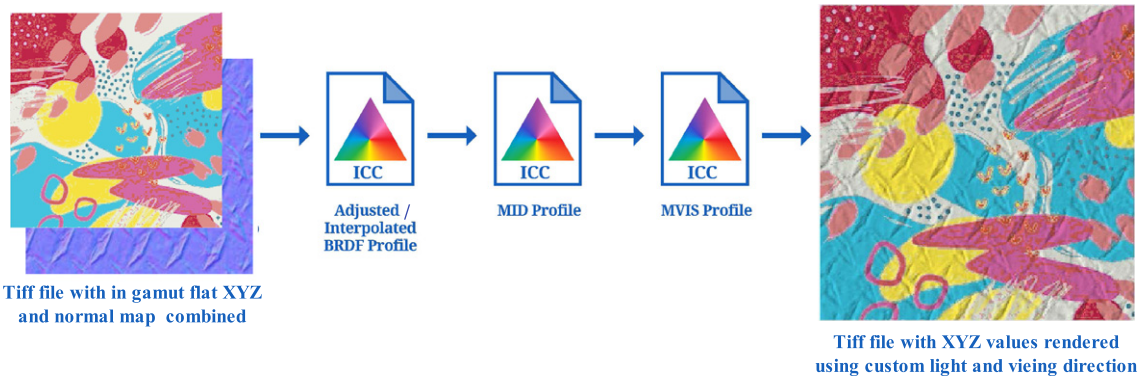

Figure 7. A practical appearance reproduction framework for softproofing of a printed 3D surface.

known standard colour difference formulas including ΔE^*_{00} were based on flat colour samples [14]. Ruili et al. optimised parametric factors of ΔE^*_{ab} and ΔE^*_{00} using visual results obtained for 3D printed spherical objects. Therefore in the future for assessments, such a 3D colour difference metric will be considered for assessment.

AIB/IB workflow can be encoded into an ICC profile using iccMAX, and using the BRDF rendering through an MCS profile workflow, material appearance can be reproduced for any global light and viewing direction passed at run-time to this colour management pipeline. This framework also requires a file format to include the BRDF parameters and the surface normals; therefore, it would be important to find a standard way of communicating rendering parameters. Psychophysical experiments are also required to evaluate the appearance reproduction framework in the simulation of real-world objects. Further, integrating this framework into colour management can be useful for softproofing of 3D printed surfaces using 2.5D printing, a step towards a more consistent and standard way of appearance reproduction.

ACKNOWLEDGMENT

This project has received funding from the European Union's Horizon 2020 research and innovation programme under the Marie Skodowska-Curie grant agreement No. 814158. We also thank Clemens Weijkamp from Canon, Venlo for providing us with the 2.5D printed target samples and ApPEARS ESR 10 Donatela Saric from FOGRA for carrying out the reference BRDF measurements of all the printed samples.

REFERENCES

[1] M. Page, G. Obein, C. Boust, and A. Razet, "Adapted modulation transfer function method for characterization and improvement of 3d printed surfaces," Electron. Imaging **29**, 92–100 (2017).

[2] T. P. Van Song, C. Andraud, and M. V. Ortiz-Segovia, "Towards spectral prediction of 2.5d prints for soft-proofing applications," *2016 Sixth Int'l. Conf. on Image Processing Theory, Tools and Applications (IPTA)* (IEEE, Piscataway, NJ, 2016), pp. 1–6.

[3] T. Weyrich, J. Lawrence, H. P. A. Lensch, S. Rusinkiewicz, and T. Zickler, "Principles of appearance acquisition and representation," Found. Trends® Comput. Graph. Vis. **4**, 75–191 (2009).

[4] I. Tastl, M. A. Lopez-Alvarez, A. Ju, M. Schramm, J. Roca, and M. Shepherd, "A soft-proofing workflow for color 3d printing-addressing needs for the future," Electron. Imaging **2019**, 479-1 (2019).

[5] M. Piovarci, M. Foshey, V. Babaei, S. Rusinkiewicz, W. Matusik, and P. Didyk, "Towards spatially varying gloss reproduction for 3d printing," ACM Trans. Graph. **39**, 1–13 (2020).

[6] T. Habib, P. Green, and P. Nussbaum, "BRDF rendering by interpolation of optimised model parameters," *Proc. IS&T CIC28: Twenty-Eighth Color and Imaging Conf.* (IS&T, Springfield, VA, 2020), pp. 162–168.

[7] T. Habib, P. Green, and A. Sole, "Implementing directional reflectance in a colour managed workflow," *Proc. London Imaging Meeting* (IS&T, Springfield, VA, 2020), Vol. 1, pp. 119–123.

[8] R. L. Cook and K. E. Torrance, "A reflectance model for computer graphics," ACM Trans. Graph. **1**, 7–24 (1982).

[9] R. Montes and C. Ureña, "An overview of BRDF models," Technical Report LSI-2012-001, University of Grenada (2012).
[10] M. da Silva Nunes, F. M. Nascimento, G. F. Miranda Jr, and B. T. Andrade, "Techniques for brdf evaluation," Vis. Comput. **38**, 573–589 (2022).
[11] ICC. "Specification ICC.1:2022 Image technology colour management — architecture, profile format, and data structure," *Int'l. Color Consortium* (2022).
[12] ICC. "Specification ICC.2:2019 image technology colour management — extensions to architecture, profile format and data structure," *Int'l. Color Consortium* (2019).
[13] "iccMAX multi processing element calculator programming," Technical Report, Int'l. Color Consortium (2018).
[14] R. He, K. Xiao, M. Pointer, M. Melgosa, and Y. Bressler, "Optimizing parametric factors in cielab and ciede2000 color-difference formulas for 3d-printed spherical objects," Materials **14**, 4055 (2022).